UNIVERSITY OF BIRMINGHAM
University of Birmingham Research at Birmingham

# Dynamic Reconfiguration of Brain Functional Network in Stroke

Wu, Kaichao; Jelfs, Beth; Neville, Katrina; Mahmoud, Seedahmed S.; He, Wenzhen; Fang, Qiang

*DOI:*
10.1109/JBHI.2024.3371097

*License:*
Creative Commons: Attribution-NonCommercial-NoDerivs (CC BY-NC-ND)

*Document Version*
Peer reviewed version

*Citation for published version (Harvard):*
Wu, K, Jelfs, B, Neville, K, Mahmoud, SS, He, W & Fang, Q 2024, 'Dynamic Reconfiguration of Brain Functional Network in Stroke', *IEEE Journal of Biomedical and Health Informatics* .
https://doi.org/10.1109/JBHI.2024.3371097

Link to publication on Research at Birmingham portal

**General rights**
Unless a licence is specified above, all rights (including copyright and moral rights) in this document are retained by the authors and/or the copyright holders. The express permission of the copyright holder must be obtained for any use of this material other than for purposes permitted by law.

•Users may freely distribute the URL that is used to identify this publication.
•Users may download and/or print one copy of the publication from the University of Birmingham research portal for the purpose of private study or non-commercial research.
•User may use extracts from the document in line with the concept of 'fair dealing' under the Copyright, Designs and Patents Act 1988 (?)
•Users may not further distribute the material nor use it for the purposes of commercial gain.

Where a licence is displayed above, please note the terms and conditions of the licence govern your use of this document.

When citing, please reference the published version.

**Take down policy**
While the University of Birmingham exercises care and attention in making items available there are rare occasions when an item has been uploaded in error or has been deemed to be commercially or otherwise sensitive.

If you believe that this is the case for this document, please contact UBIRA@lists.bham.ac.uk providing details and we will remove access to the work immediately and investigate.

Download date: 07. May. 2024

This article has been accepted for publication in IEEE Journal of Biomedical and Health Informatics. This is the author's version which has not been fully edited and content may change prior to final publication. Citation information: DOI 10.1109/JBHI.2024.3371097



# Dynamic Reconfiguration of Brain Functional Network in Stroke

Kaichao Wu, Beth Jelfs, Katrina Neville, Seedahmed S. Mahmoud, Wenzhen He* and Qiang Fang*

***Abstract*— The brain continually reorganizes its functional network to adapt to post-stroke functional impairments. Previous studies using static modularity analysis have presented global-level behavior patterns of this network reorganization. However, it is far from understood how the brain reconfigures its functional network dynamically following a stroke. This study collected resting-state functional MRI data from 15 stroke patients, with mild (n = 6) and severe (n = 9) two subgroups based on their clinical symptoms. Additionally, 15 age-matched healthy subjects were considered as controls. By applying a multilayer temporal network method, a dynamic modular structure was recognized based on a time-resolved function network. The dynamic network measurements (recruitment, integration, and flexibility) were calculated to characterize the dynamic reconfiguration of post-stroke brain functional networks, hence, revealing the neural functional rebuilding process. It was found from this investigation that severe patients tended to have reduced recruitment and increased between-network integration, while mild patients exhibited low network flexibility and less network integration. It's also noted that previous studies using static methods could not reveal this severity-dependent alteration in network interaction. Clinically, the obtained knowledge of the diverse patterns of dynamic adjustment in brain functional networks observed from the brain neuronal images could help understand the underlying mechanism of the motor, speech, and cognitive functional impairments caused by stroke attacks. The present method not only could be used to evaluate patients' current brain status but also has the potential to provide insights into prognosis analysis and prediction.**

***Index Terms*— Dynamics, fMRI, Functional network, Stroke;**

## I. Introduction

STROKE is a common neurological disorder that can significantly impair cognitive and motor functions. Nevertheless, due to brain plasticity, the stroke brain can adjust its network architecture to adapt to structural damage and compensate for the lost functions [1], [2]. The brain functions are fulfilled by a set of functionally specialized modules, i.e., distributed brain regions that interact and cooperate with each other, either within modules or between modules, in response to the functional demands of the external environment [3], [4]. Therefore, the altered functional network of the stroke brain implies that it is reconfiguring its modular structure to support the post-stroke plasticity [5].

In this regard, functional neuroimaging data, particularly resting-state functional MRI, have contributed enormously to understanding the reorganization mechanisms of network modules underpinning post-stroke plasticity and brain adaptability [6]–[8]. A frequent observation is the reduction of the functional network's modularity after a stroke [9]–[12]. Modularity is a graph measure of how well a network can be divided into smaller modules that describes the structure of the network [13]. This reduction in modularity reflects the decreased segregation between different functional domains and integration within domains, to some extent explaining the post-stroke clinical deficits [11], [14]. The reduced modularity usually lasts a few weeks to a month after the stroke, following which the modular brain network gradually recovers, in parallel with the functional improvement (e.g., improvements in language [9] and attention [15]).

Nevertheless, of note that these findings typically rest on a static representation or a single brain network built from an entire resting-state functional MRI scan. Recently, dynamic functional network connectivity analysis (DFNC) has recently gained popularity due to its capacity to delineate spontaneous variation of functional connectivity [16]–[19]. Hence, while static construction is valuable and productive, the growing body of DFNC studies on time-varying networks suggests that the temporal dynamics of the modular brain should be assessed [20], [21]. In addition, the time dependence of the modularity recovery implies that the dynamic reconfiguration of the brain networks could be the root source of decreased or increased static modularity thus further emphasizing the need to evaluate post-stroke module dynamics. Furthermore, the brain's dynamic reconfiguration has been proven to be a promising avenue for creating novel biomarkers of diseases, such as attention-deficit/hyperactivity disorder [22] schizophrenia [23], temporal lobe epilepsy [24] and depression [25]. However, if and how the brain network dynamically reconfigures itself following a focal stroke, particularly under different levels of clinical severity, remains not fully understood.

This work was supported by the Li Ka Shing Foundation Cross-Disciplinary Research Grant (2020LKSFG01C). The asterisk indicates the corresponding authors.

Kaichao Wu, Seedahmed S. Mahmoud *Qiang Fang are with the Department of Biomedical Engineering, College of Engineering, Shantou University, Shantou, China (e-mail: {kaichaowu, qiangfang}@stu.edu.cn).

Kaichao Wu and Katrina Neville are with the School of Engineering, RMIT University, Melbourne, Australia (e-mail: katrina.neville@rmit.edu.au).

Beth Jelfs is with the Department of Electronic, Electrical, and Systems Engineering, University of Birmingham, Birmingham, UK. (e-mail: b.jelfs@bham.ac.uk.)

*Wenzhen He is with the First Affiliated Hospital of Shantou University Medical College, China (e-mail: wenzhen_he@sina.com).

This work is licensed under a Creative Commons Attribution-NonCommercial-NoDerivatives 4.0 License. For more information, see https://creativecommons.org/licenses/by-nc-nd/4.0/

This article has been accepted for publication in IEEE Journal of Biomedical and Health Informatics. This is the author's version which has not been fully edited and content may change prior to final publication. Citation information: DOI 10.1109/JBHI.2024.3371097



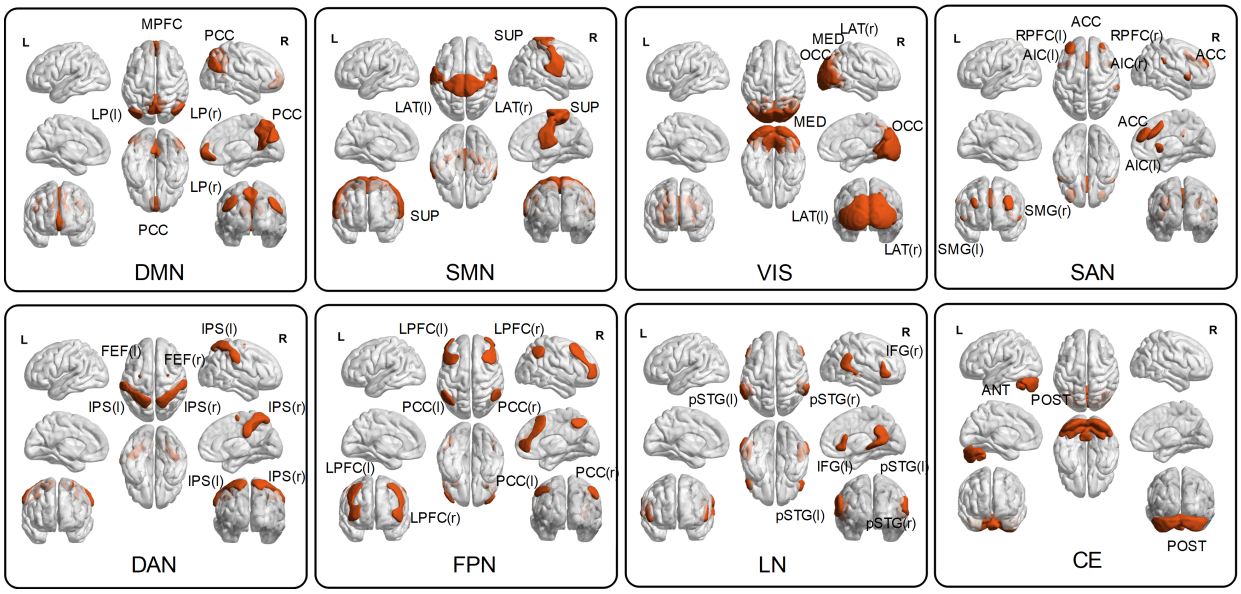


Fig. 1. Spatial mapping of predefined 32 ROIs and 8 corresponding networks for multilayer dynamic analysis. Default mode network (DMN): the medial prefrontal cortex (MPFC), precuneus cortex (PCC), bilateral lateral parietal (LP); sensorimotor network (SMN): superior, bilateral lateral; visual network (VIS): medial, occipital, bilateral lateral; salience network (SAN): anterior cingulate cortex (ACC), bilateral anterior insula (AI), rostral prefrontal cortex (RPFC), and supramarginal gyrus (SMG); dorsal attention network (DAN): bilateral frontal eye field (FEF) and intraparietal sulcus (IPS); frontoparietal network (FPN): the bilateral lateral prefrontal cortex (LPFC) and posterior parietal cortex (PPC); language network (LN): bilateral inferior frontal gyrus (IFG) and posterior superior temporal gyrus (pSTG); and cerebellar network (CE): anterior, posterior.

Therefore, this study investigated the dynamic reconfiguration of functional brain networks in stroke patients with different degrees of clinical symptoms. We hypothesize that the post-stroke brain dynamic readjusts its functional network topology according to clinical severity. The hypothesis is twofold: first, the brain functional network of stroke patients undergoes dynamic changes. If these changes do happen, they can be evidenced by highly significant alterations in the measurements that characterize dynamic reconfiguration following a stroke. Second, the dynamic behaviors of the brain functional network exhibit highly significant alteration between subgroups, i.e., reconfiguration pattern differs between patients with distinct degrees of clinical symptoms.

To verify this hypothesis, the brain fMRI data from 15 stroke subjects with two degrees of clinical severity (mild: 6 and severe: 9) and 15 age-matched healthy controls were analyzed with the help of the developed multilayer network model [6]. The results demonstrate that the post-stroke human brain reorganizes its functional networks to adapt to stroke damage. This network reconfiguration after stroke will also be modulated according to the degree of stroke attacks. Besides, the static network exhibits differences across patients with different levels of severity; however, it cannot reflect the dynamic process of the brain network adjusting itself to compensate for the functional injuries. Together, these results reveal the brain dynamic behaviors in seconds and shed new light on the mechanisms underlying post-stroke brain network reorganization.

## II. Materials and Methods

TABLE I
DEMOGRAPHICS AND CLINICAL CHARACTERISTICS OF PARTICIPANTS.

| | Stroke patients (n = 15) | Healthy controls (n = 15) | P-value |
|---|---|---|---|
| Age, years | 63.8 (47-81) | 68.6 (61-81) | 0.18 |
| Sex, %female | 4 | 7 | 0.17 |
| Mean FD | 0.033 (0.01-0.05) | 0.088 (0.02-0.11) | 0.99 |
| Days since stroke | 23.06 (14-42) | — | — |
| NIHSS | 7.26 (1-20) | — | — |
| Lesion volume(ml) | 13.01 (0.91, 63.55) | — | — |

Values are presented as mean (range) unless otherwise stated. FD: framewise displacement

### A. Participants

The stroke samples examined in this study were from fifteen ischemic stroke patients admitted to the 1st affiliated hospital of Shantou University Medical College (SUMC, mean age 63.8 years with a standard deviation of 11.68 years, 4 male/11 females, mean day of MRI scan post-stroke is 23.06 with a standard deviation of 4.32). The patients were recruited from a study approved by the medical research ethics committees of the named hospitals, and all participants signed informed consent.

Patients with the National Institutes of Health Stroke Scale (NIHSS)>5 were assigned to a severe subgroup; otherwise, they were assigned to the mild subgroup [26]. In addition, fifteen age-matched healthy samples from our previous research served as control groups [27] (7 male and 8 female, mean age 68.6 years with a standard deviation of 6.4 years). Demographics and clinical characteristics of participants can be seen in Table I.

This work is licensed under a Creative Commons Attribution-NonCommercial-NoDerivatives 4.0 License. For more information, see https://creativecommons.org/licenses/by-nc-nd/4.0/

This article has been accepted for publication in IEEE Journal of Biomedical and Health Informatics. This is the author's version which has not been fully edited and content may change prior to final publication. Citation information: DOI 10.1109/JBHI.2024.3371097



### B. MRI Acquisition

MRI data were acquired on a Discovery standard 3.0 T scanner using an 8-channel head coil at the MRI center of SUMC. The high-resolution T1 anatomical images were acquired with a multi-planar rapidly acquired gradient echo sequence with 1 mm isotropic voxels, a $256 \times 256$ matrix size, and a 9-degree flip angle (129 slices, repetition time (TR) = 2250 ms, Time of echo (TE) = 4.52 ms). With the T1, the lesion profile of all patients has been created as a lesion overlap map (the details and corresponding lesion map can be seen in Supplementary Material A).

Resting-state functional MRI was collected after the anatomical scan using single-shot gradient-echo EPI sequence: TR = 2,000 ms; TE = 30 ms; flip angle = 90; field of view = $240 \times 240$ mm$^2$; matrix size = $64 \times 64$; number of slices = 25; and voxel size = $3.43 \times 3.43 \times 5.0$ mm$^3$ with no gap; and 210 volumes acquired in 7 min.

### C. FMRI Data Preprocessing and Head Motion Control

The functional MRI scans were processed using a customized pre-processing pipeline in the CONN functional connectivity toolbox [28] in conjunction with the Statistical Parametric Mapping software package (SPM12) [29]. For all subjects, the first 10 functional volumes were removed to eliminate the effects of unstable magnetization and thus to obtain a steady blood oxygenation level-dependent activity signal. The remaining 200 images were corrected for slice timing and head motion and then normalized to Montreal Neurologic Institute (MNI) space. The non-smoothed functional images were finally fed into the default denoising pipeline to eliminate confounding effects and temporal band-pass filtering.

The head motion effect was controlled in functional connectivity analysis by calculating the individual framewise displacements (FD). Participants with a maximum displacement exceeding 1.5 mm and a maximum rotation above 1.5 degrees were excluded. In practice, no subjects exceeded these criteria, so non were excluded. In addition, 24 motion parameters, calculated from the six original motion parameters, were regressed out as nuisance covariates. Finally, there was no significant group difference in mean FD when comparing the 15 stroke patients with the 15 healthy controls.

### D. Functional Connectivity Estimation

Functional connectivity is estimated by calculating the Person's correlation coefficient between pairwise time series of spatially distinct brain regions. These regions are generated from anatomically or functionally parcelled brains, also known as brain parcels [22]. This study used a functional brain parcellation provided by CONN to investigate the changing network configuration due to stroke lesions. This parcellation runs from CONN's group ICA (independent component analysis) of the HCP dataset (497 subjects) which comprises 32 regions of interest (ROIs), covering the whole-brain area and being formed by eight large-scale networks/systems (details can be seen in Fig. 1). The set of ICA spatial maps can be mapped onto each subject's fMRI BOLD data to derive one representative timeseries per ROI. Then, for $N$ ROIs, a $N \times N$ functional connectivity matrix $A$ can be created, where each entry $A_i$ is a pairwise Person's coefficient between ROIs $i$ and $j$. To eliminate the bias, Fisher's Z-transformation was applied to the functional connectivity matrices to obtain normally distributed Z-scores, and only the positive values were retained in the further connectivity analysis.

### E. Static Modularity

Static modularity is a theoretical graph metric measuring the segregation between distinct brain function systems [30]. As suggested in previous studies [10], [31], Newman's method was implemented in the Brain Connectivity Toolbox for the static modularity calculation [32]. Considering that simply binarizing the network with a threshold value might cause the loss of information of rich community structure, static modularity was calculated at edge densities ranging from 4 to 20% with the symmetric treatment of negative weights that are consistent with references [10], [31], [33]. The modularity calculated at each edge density was tested to see if there were significant differences between subgroups (mild vs. severe, severe vs. control, mild vs. control). To eliminate the bias that results from differences in correlation magnitudes across individuals, the average values across densities with a significant group effect were used as the final static modularity.

### F. Multilayer Modularity

The multilayer modularity analysis was conducted on each subject with the following steps (the detailed flowchart can be seen in Fig. 2):

**Dynamic functional connectivity estimation**. Multilayer modularity calculation for dynamics analysis starts with dynamic functional network connectivity (DFNC) estimation. The BOLD time series extracted from the denoised fMRI data were first processed with a common sliding window scheme to obtain temporal slices (see Fig. 2A). The tapered window was used, which was obtained by convolving a rectangle (equal to the window size) with a Gaussian ($\sigma$ = 3). While the optimal choice of window width setting in the sliding window scheme is still under debate, prior studies have provided evidence that the number of communities fluctuates narrowly with a window width of 100s (50 TR) [4], [34]. In this paper, the window width was opted for 50 TR and a step size of 1 TR [35](The alternative option with a window width of 20 TR has been shown in Supplemental Material C). By calculating the pairwise Pearson's correlation coefficient of time series within a window, the sliding windows formed a series of functional connectivity matrixes, and then Fisher's z-transform was applied to these matrixes to estimate the time-varying functional connectivity of the brain network.

**Multilayer modular network detection**. Using the time-varying functional network estimated by DFNC, a multilayer modular network can be detected as follows: first, the dynamical functional connectivity matrices of stroke patients and healthy controls were concatenated along the diagonal to produce their initial community profile (obtaining a matrix with $4,768 \times 4,768$, where $4,768 = 149 \times 32$, being the number

This work is licensed under a Creative Commons Attribution-NonCommercial-NoDerivatives 4.0 License. For more information, see https://creativecommons.org/licenses/by-nc-nd/4.0/

This article has been accepted for publication in IEEE Journal of Biomedical and Health Informatics. This is the author's version which has not been fully edited and content may change prior to final publication. Citation information: DOI 10.1109/JBHI.2024.3371097



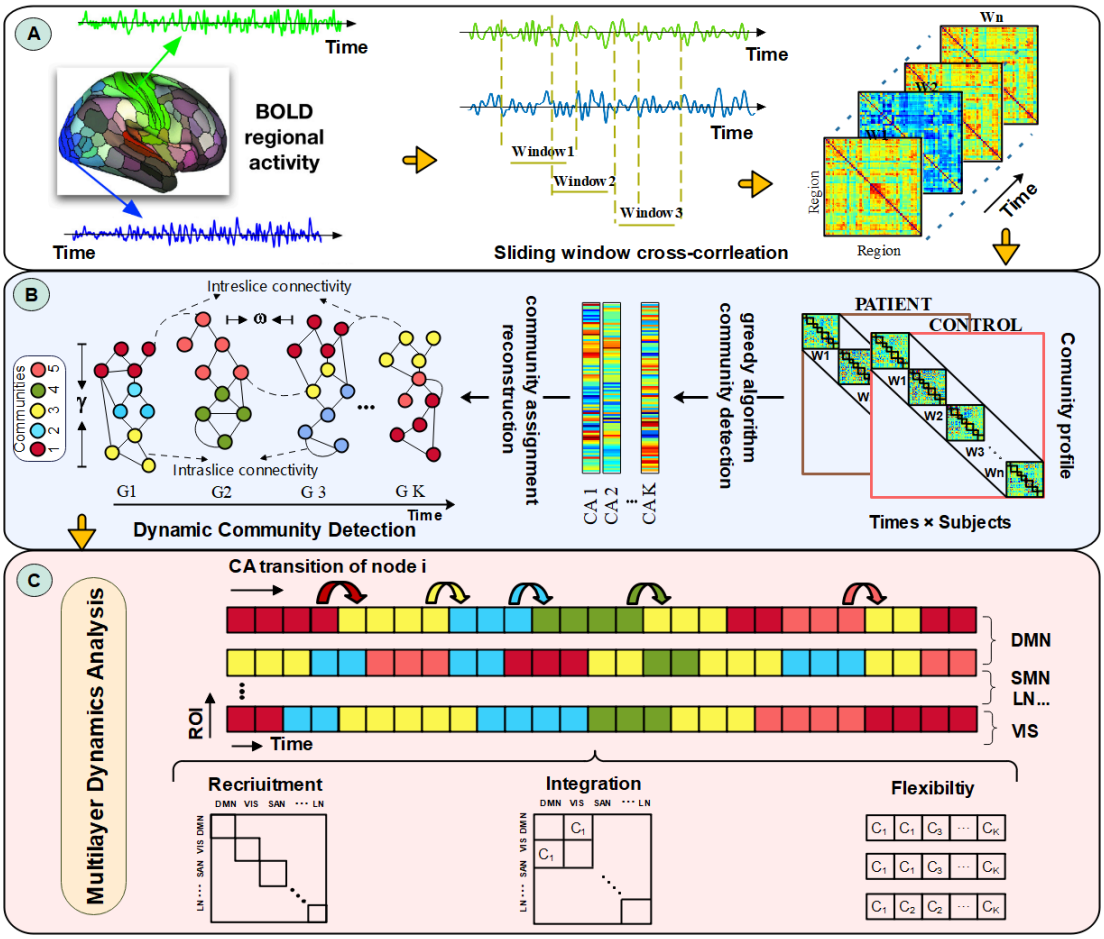


Fig. 2. Flowchart of the multilayer dynamics analysis framework. **A. Dynamic functional connectivity estimation**: the regional BOLD signal extracted from denoised fMRI data was decomposed by a sliding window, forming a time-varying function network.**B. Multilayer temporal network detection**: The estimated time-varying function network matrixes per subject, including patients and healthy controls, were connected to generate the initial module profile; next greedy algorithm was applied for community detection, through maximizing a multilayer modularity maximization function. The generated community assignments (CA) were then projected to the original functional connectivity matrixes to reconstruct the graph representation of the functional network with a time-varying module structure; **C. Multilayer dynamics analysis:** three measurements characterizing the network reconfiguration were finally computered. The arrows indicate the direction of data flow.

of sliding windows and the size of each window respectively). Then, a Louvain-like greedy community detection algorithm was applied to each subject's initial profile for dynamic community optimization introduced by [36]. Specifically, for each subject, this algorithm optimizes the multilayer modularity partition by maximizing the modularity quality function, which is defined as:

$$Q_M = \frac{1}{2\mu} \sum_{ijlr} \left[ \left( A_{ijl} - \gamma_l M_{ijl} \right) \delta_{lr} + \delta_{ij} \omega_{jlr} \right] \delta \left( g_{il}, g_{jr} \right), \tag{1}$$

where

- $A_{ijl}$ is the weight of the edges between nodes $i$ and $j$ at layer $l$;
- $M_{ijl}$ is the connection expected in the created null model, which is defined by the widely used Newman-Girvan null model [4].
- $M_{ijl} = \frac{k_{il} k_{jl}}{2m_l}$, where $k_{jl}$ is the weighted degree of node $j$ in layer $l$, that is the sum of the weights of the edges connected to node $j$ in layer $l$;
- $m_l$ is the total nodal weighted degrees in layer $l$;
- $\mu = \frac{1}{2} \sum_{ij} \left( k_{jr} + c_{jr} \right)$ is the sum of the weights of the dynamic functional connectivity matrix;
- $c_{jr} = \sum_l \omega_{jrl}$ and $\omega_{jrl}$ defines the inter-slice connections which is the connection strength between node $j$ in layer $l$ and node $j$ in layer $r$.
- $\delta_{ij}$ denotes the Kronecker $\delta$-function, where $\delta_{ij} = 1$ if $i = j$, otherwise 0;
- $g_{il}$ and $g_{jr}$ represent the community node $i$ is assigned to in layer $l$ and node $j$ in layer $r$ respectively;
- $\delta \left( g_{il}, g_{jr} \right) = 1$ if $g_{ir} = g_{jl}$, otherwise 0;

The parameters $\gamma$ and $\omega$ are the intra-layer and inter-layer coupling parameters, controlling the number of modules detected in layers and across layers. Inspired by [4], [15], [35], a grid-search method was used to find the optimal $\gamma - \omega$ pair across the range of $\gamma \in [0.9, 1.0, 1.1]$ and $\omega \in [0.5, 0.75, 1.0]$ to maximize the dynamic modularity. The results of the choice of these two parameters can be seen in Supplementary Material(B). Finally, the final values of the two hyperparameters were determined to be 0.9 and 1.0 respectively.

The final optimization associates the modularity partition information to each sliding window. Hence, for the 149 sliding

This work is licensed under a Creative Commons Attribution-NonCommercial-NoDerivatives 4.0 License. For more information, see https://creativecommons.org/licenses/by-nc-nd/4.0/

This article has been accepted for publication in IEEE Journal of Biomedical and Health Informatics. This is the author's version which has not been fully edited and content may change prior to final publication. Citation information: DOI 10.1109/JBHI.2024.3371097



windows of each subject obtained in the multilayer resolution, there would be 149 community assignment ($CA$) vectors; the length of each $CA$ vector is $N$, corresponding to the number of predefined ROIs, and the value of the $CA$ vector represents the community that ROI assigned. The obtained $CA$ vectors were then projected to the time-varying functional connectivity network to construct graph matrixes $\mathcal{G} = \left\{\mathcal{G}_i^{CA_i}\right\}_{i=1}^{n}$. $n$ is the number of sliding windows and $\mathcal{G}_i \in \mathbb{R}^{N\times N}$ is the graph representation of the function connectivity matrix at timepoint $i$, indicating the functional connectivity network with time-varying module structure. After reconstruction, a multilayer modular network with a complex and rich community modularity structure spanning the time-varying layers can be obtained (see Fig. 2 B for the flowchart).

**Multilayer temporal dynamics analysis.** For each participant from the two different subgroups, three temporal measurements: recruitment, integration, and flexibility, were calculated to characterize the multilayer network dynamics based on the detected dynamic community structure (Fig. 2 C).

Recruitment and integration quantify the alteration of dynamic functional interaction within and between brain functional systems. Precisely, recruitment is measured by the fraction of layers in which ROIs from the same functional system are assigned to the same community [10]. The recruitment of a given predefined functional system $S$ is defined as:

$$R_S = \frac{1}{n_S}\sum_{i\in S}\sum_{j\in S} P_{ij}, \tag{2}$$

where $n_S$ is the number of ROIs belonging to the system $S$; $P_{ij}$ is the allegiance matrix of the multilayer modular networks, which is defined as :

$$P_{ij} = \frac{1}{T}\sum_{t=1}^{T} a_{ij}^{t} \tag{3}$$

$a_{ij}^{t} = 1$ if in layer $t$ nodes $i$ and $j$ are assigned to the same community, and 0 otherwise. Similar to recruitment, the integration of a given predefined functional system $S$ is defined as:

$$I_S = \frac{1}{N - n_S}\sum_{i\in S}\sum_{j\notin S} P_{ij}. \tag{4}$$

The system of interest is highly functionally integrated when its functional regions are frequently assigned to the same community as other regions. Therefore, to quantify this, an integration coefficient can also be defined between different functional systems [37]. The integration between functional system $S_k$ and $S_l$ is calculated as:

$$I_{S_kS_l} = \frac{1}{n_{S_k}n_{S_l}}\sum_{i\in S_k}\sum_{j\in S_l} P_{ij}. \tag{5}$$

The higher the between-system integration, the stronger the functional coordination between systems. This study investigated both within-system and between-system integration alterations caused by stroke lesions.

Flexibility characterizes the community stability of a system in multilayer resolution [11]. The flexibility of a system corresponds to the average number of times that its brain regions change module allegiance. The system $S$'s flexibility is defined as:

$$F_S = \frac{1}{n_s \times (T-1)}\sum_{i\in S}\sum_{t=1}^{T} b_i, \tag{6}$$

where $n_S$ is the number of regions belonging to the system $S$, $T$ is the multilayer resolution, and $b_i = 1$ if in the next layer $t+1$ the node $i$ is assigned to a different community.

Noting that random effects in the Louvain-like greedy community detection algorithm exist in multilayer community detection [36], the multilayer modularity optimization was run 100 times for each subject. The mean of the corresponding dynamic measures from the 100 repetitions served as their final values. Besides, a rewiring approach [20], [38] was used for the normalization of these dynamic measures. Specifically, a null distribution was created from 1000 randomly rewired function connectivity matrices. The recruitment, integration, and flexibility are then divided by the mean of corresponding measurements calculated from the null distribution(z-score ¿2)to obtain normalized values.

### G. Statistical Analysis

A 2-sample t-test (control covariates: age, sex, and FD ) was performed on the static functional connectivity and modularity to determine if there were functional network changes between patient groups and controls. In addition, a three-level one-way ANOVA (level of significance $p < 0.05$) was performed to investigate if there were static modularity differences in healthy controls and mild and severe patients. In case of significant ANOVA results, post hoc t-tests (mild patients, severe patients, and controls) were performed. Correction for multiple comparisons was always applied whenever testing more than one hypothesis simultaneously (false discovery rate (FDR) correction $p < 0.05$).

## III. Results

### A. Whole Brain Static Modularity Alteration

Fig. 3 shows the static modularity for each group and each density. As expected, the edge density also has significant effects on the whole brain functional network modularity ($F(16) = 28.63$, $p < 0.0001$). Comparing the different edge densities, at only 5 densities, was the modularity significantly different between mild, severe, and control subgroups ($p_{0.04} = 0.011$, $p_{0.05} = 0.009$, $p_{0.06} = 0.014$, $p_{0.07} = 0.008$, $p_{0.08} = 0.014$). In general, the stroke patients had much lower functional network modularity ($F(2) = 47.25$, $p < 0.0001$), suggesting that the brain tends to have a less segregated functional network after stroke. The final static modularity also indicates that both the mild patients ($p = 0.02$, Bonferroni corrected) and the severe patients ($p = 0.04$, Bonferroni corrected) have lower network segregation than healthy controls. However, the significant effect on the static modularity was not detectable between the groups of mild and severe patients.

This work is licensed under a Creative Commons Attribution-NonCommercial-NoDerivatives 4.0 License. For more information, see https://creativecommons.org/licenses/by-nc-nd/4.0/

This article has been accepted for publication in IEEE Journal of Biomedical and Health Informatics. This is the author's version which has not been fully edited and content may change prior to final publication. Citation information: DOI 10.1109/JBHI.2024.3371097



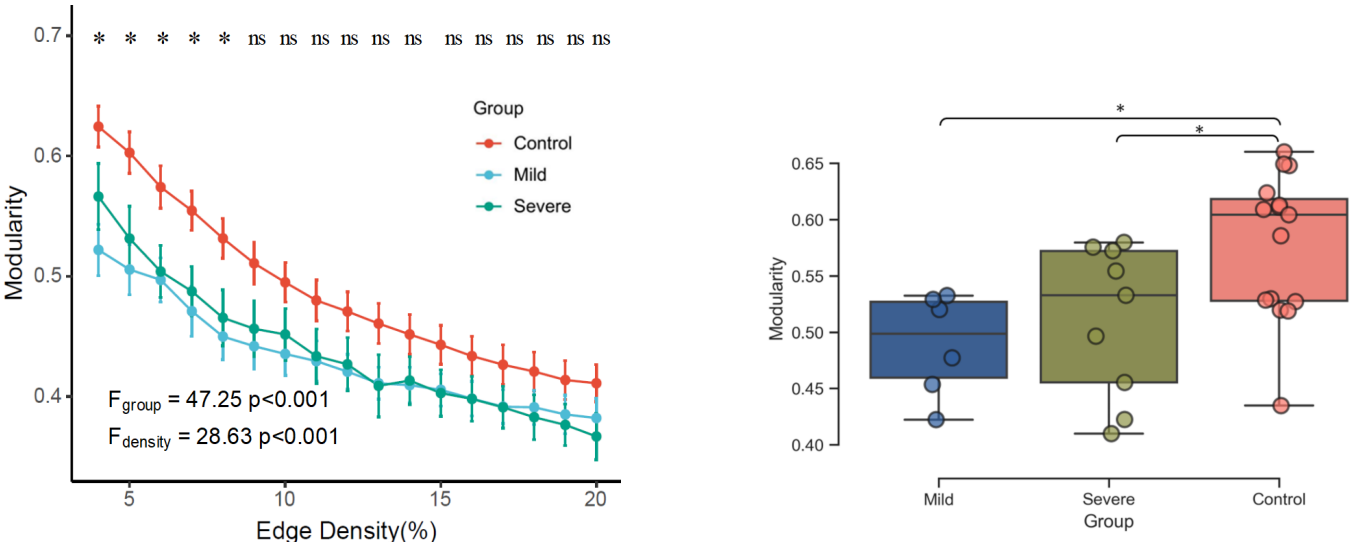


Fig. 3. The static modularity alteration. **Left**. Modularities across edge densities are shown for mild, severe, and healthy controls. Dots represent the mean value; error bars represent 95% confidence intervals, **Right.** The final static modularity difference between different subgroups; horizontal lines indicate group means, and asterisks represent significant differences at $p < 0.05$ Bonferroni corrected, $ns$ denotes no significance.

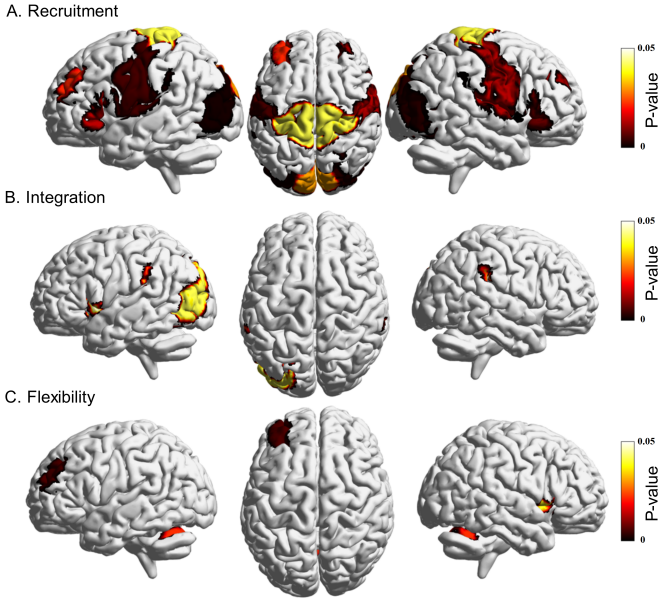


Fig. 4. Brain regions exhibiting significant differences in ANOVA results for A. recruitment, B. integration, and C. flexibility. The colorbar indicates the range of $p-$value. The deeper the color the less the $p-$value.

## B. Significant Brain Region Reconfiguration

Static modularity reflects the average state that functional brain networks exhibit. However, the modular organization is not static but instead fluctuates constantly in response to the brain's functional demands, especially demands that have dramatic changes, such as when facing brain deficits. Three measures were produced to characterize this dynamic process based on the detected multilayer modular network. Fig. 4 shows the brain regions with significant differences in these measurements using three-level one-way ANOVA analysis results. According to the network parcellation, those brain regions with significant differences in recruitment are distributed across four networks: SMN, SAN, VIS, and LN (Fig. 4A, refer to Fig. 1 for their definitions and brain location.). The brain regions with significant differences in integration mainly reside in SAN and VIS (Fig. 4B). Brain regions with significant differences in flexibility are distributed primarily in network SAN and CE (Fig. 4C).

## C. Trends in Network Reconfiguration Based on Stroke Severity

The brain regions which showed significantly different measurements between groups imply that the brain networks reconfigure themselves after stroke. Next, we examined how dynamic reconfiguration is exhibited in brain functional networks and whether these configuration patterns differ between patients with different stroke severity.

First, the between-group differences in recruitment are examined. The mild and severe patients show that most brain regions decline in recruitment compared to healthy controls. Severe patients exhibit more regions with declined recruitment compared to healthy controls than do the mild patients, implying that the number of regions with decreased recruitment increases as stroke severity grows. This inference was reinforced when solely comparing mild patients and severe patients, where the severe patients showed lower recruitment in ACC ($t = -2.225$, $p = 0.044$), left anterior insula ($t = 2.664$, $p = 0.019$) and right SMG ($t = -2.546$, $p = 0.024$) than the mild patients. Fig. 5 illustrates the distribution of these regions with significant differences between subgroups. As nodal-level recruitment significantly differs, so the recruitment in large-scale systems exhibits differences ($F = 15.29$ $p < 0.0001$). Post hoc comparison shows the mild patients had lower recruitment in VIS ($t = -4.973$, $p < 0.0001$) and LN ($t = -2.342$, $p = 0.030$), and the severe patients in SMN, SAN and LN compared to healthy controls (FDR corrected $p < 0.05$).

Next, the group difference in integration between controls, mild patients, and severe patients was tested with the results

This work is licensed under a Creative Commons Attribution-NonCommercial-NoDerivatives 4.0 License. For more information, see https://creativecommons.org/licenses/by-nc-nd/4.0/

This article has been accepted for publication in IEEE Journal of Biomedical and Health Informatics. This is the author's version which has not been fully edited and content may change prior to final publication. Citation information: DOI 10.1109/JBHI.2024.3371097



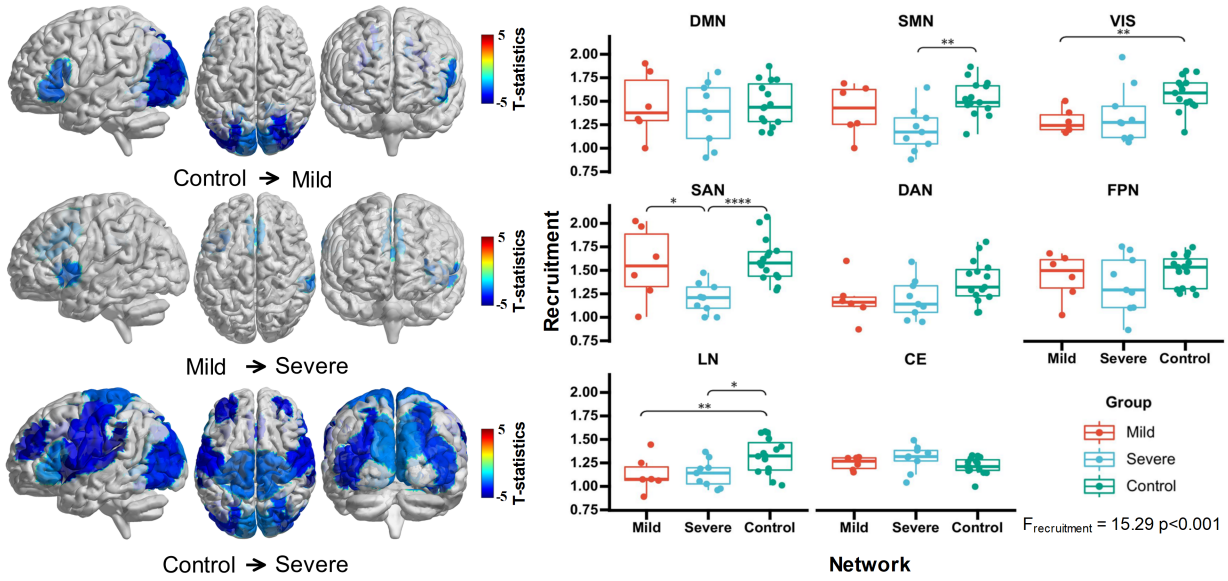


Fig. 5. Results of post-hoc tests to examine the differences in recruitment between groups with distinct clinical symptoms ($*p < 0.05$ two-sided, FDR corrected). The brain maps on the left indicate the significantly different areas between subgroups, and the color bar represents the t statistic, indicating the direction alteration. The boxplot on the right shows the network alteration between subgroups. DMN: Default mode network. SMN: sensorimotor network. VIS: Visual network. SAN: salience network. DAN: dorsal attention network. FPN: frontoparietal network. LN: language network, CE: cerebellar network.

shown in Fig. 6. The post hoc comparison indicates that severe patients have higher integration in the anterior insula ($t = 2.762$, $p = 0.011$), right and left SMG (left: $t = 2.886$, $p = 0.009$. right: $t = 2.869$, $p = 0.009$), and lateral visual area ($t = 2.618$, $p = 0.016$) compared to controls. Neither mild patients and controls nor mild patients and severe patients differed in this aspect. In terms of integration between brain functional networks, the integration between DMN and CE ($F = 4.54$, $p = 0.019$), SMN and CE ($F = 3.66$, $p = 0.039$), VIS and LN ($F = 4.18$, $p = 0.026$), DAN and CE ($F = 4.71$, $p = 0.017$), FPN and CE ($F = 3.45$, $p = 0.04$) was significantly altered. Post hoc t-tests, contrasting mild patients and healthy controls, revealed a stroke-induced decrease in integration between DMN and CE ($t = -2.124$, $p = 0.036$) but an increase between VIS and LN ($t = 2.208$, $p = 0.040$), DAN and CE ($t = 2.757$, $p = 0.013$). In contrast, severe patients comprised a decrease in integration between DMN and CE ($t = -2.653$, $p = 0.015$), FPN and CE ($t = -2.899$, $p = 0.008$), but an increase between SMN and CE ($t = 3.345$, $p = 0.003$), VIS and LN ($t = 2.213$, $p = 0.037$), and DAN and CE ($t = 2.218$, $p = 0.037$) when compared to healthy controls ($p < 0.05$, FDR-corrected). Mild and severe patients did not feature significant differences in between-network integration after correction for multiple comparisons. Fig. 6A. illustrates the details on the integration of altered network pairs.

Lastly, we investigated the between-group difference in flexibility. While a significant effect in flexibility was not detected when contrasting severe patients and healthy controls, mild patients featured significantly different flexibility in brain regions and functional networks compared to both controls and severe patients. In particular, the majority of the significantly altered areas resided in the salience and cerebellum functional domains. For example, mild patients have lower flexibility in the left RPFC than both other groups (to controls: $t = -4.078$, $p = 0.0006$; to severe patients: $t = -2.648$, $p = 0.020$). The lower flexibility in the mild patients was also exhibited in the anterior cerebellum when contrasting with controls ($t = -2.433$, $p = 0.025$) and in the right insula when contrasting with severe patients ($t = -2.039$, $p = 0.038$). A similar trend between groups is also observed in terms of functional network flexibility. Mild patients not only featured less flexibility in SAN than severe patients ($t = -2.410$, $p = 0.032$) but also lower flexibility in SAN ($t = -2.842$, $p = 0.010$) and CE ($t = -2.714$, $p = 0.035$) than controls. Notably, flexibility in SAN did not go down further as severity increased. When compared to mild patients, increased SAN flexibility was observed in severe patients. The box plot in Fig. 6B shows the two networks (SAN and CE) with significantly different flexibility. Severe patients and controls did not differ in this regard.

Collectively, patients, no matter which level of severity, show remarkably consistent reduced recruitment compared to healthy controls. This reduction seems to exhibit continuity, as lower recruitment was observed in severe patients compared to mild patients. On top of that, the post-stroke dynamic reconfiguration can be represented by pairwise network integration instead of within-network integration. The mild and severe patients shared increased DMN-CE and decreased VIS-LN and DAN-CE integration. Regarding flexibility, this dynamic network measure has a significant group difference in SAN and CE. Of note is that SAN flexibility displays a U-shaped curve as severity rises, which exhibits a converse trend against SAN recruitment.

This work is licensed under a Creative Commons Attribution-NonCommercial-NoDerivatives 4.0 License. For more information, see https://creativecommons.org/licenses/by-nc-nd/4.0/

This article has been accepted for publication in IEEE Journal of Biomedical and Health Informatics. This is the author's version which has not been fully edited and content may change prior to final publication. Citation information: DOI 10.1109/JBHI.2024.3371097



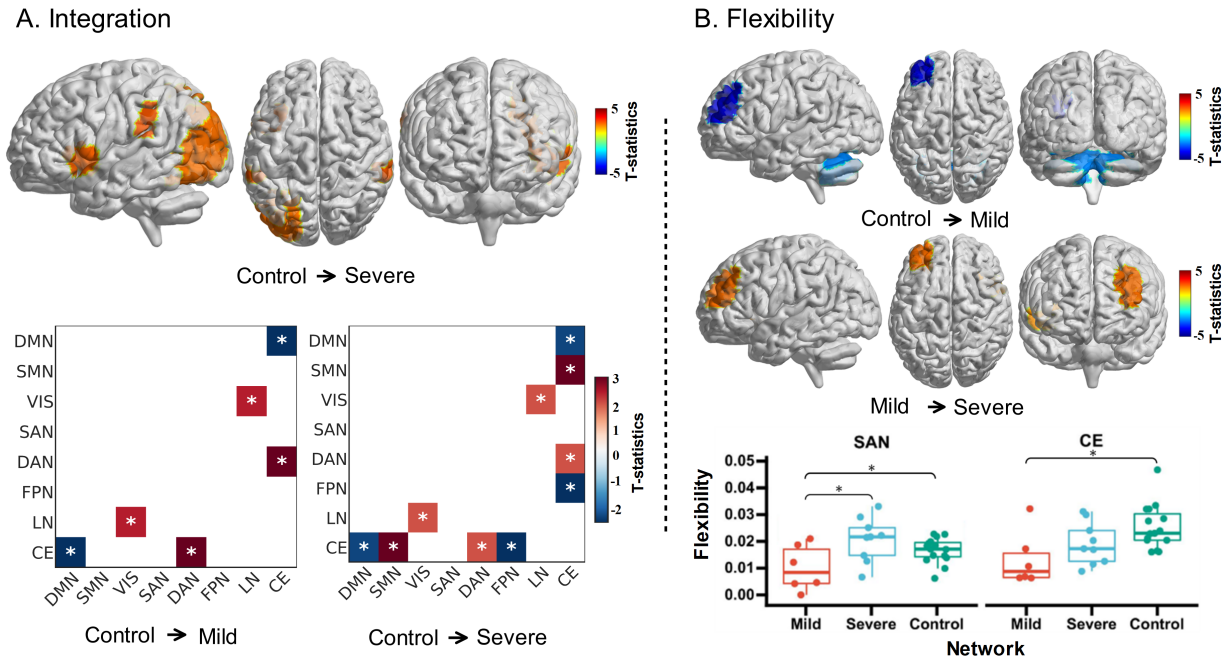


Fig. 6. Post-hoc test results examining the differences in the **(A)** integration and **(B)** flexibility between groups with distinct clinical symptoms. The brain maps indicate the significantly different areas between subgroups, and the color bar represents the t statistic, indicating the direction alteration. The colored tiles on the left in A represent between-network integration with significant effects ($*p < 0.05$ FDR corrected.). The boxplot on the right shows the network alteration between subgroups ($*p < 0.05$ FDR corrected). DMN: Default mode network. SMN: sensorimotor network. VIS: Visual network. SAN: salience network. DAN: dorsal attention network. FPN: frontoparietal network. LN: language network, CE: cerebellar network.

## IV. Discussion

In this study, the dynamic functional network changes were modeled across three groups of patients: healthy, mild stroke, and severe stroke, by using a multilayer network method. Based on the inherent dynamics of the brain in a resting state, the post-stroke multilayer function networks were constructed, and three measures (recruitment, integration, flexibility) characterizing the brain network reconfiguration after a stroke were calculated. Given the trends observed in these measures across the three states of participants, we can learn that mild and severe patients exhibit different reconfiguration patterns (a summary of the reconfiguration patterns can be seen in Fig. 7). Mild stroke patients can be summarized as having a reduction in recruitment in VIS and LN, decreased DMN-CE and increased VIS-LN and DAN-CE integration, and declined SAN and CE flexibility. In contrast, severe patients were characterized by reduced SMN, SAN, and LN recruitment. In addition to the same integration trend as in mild patients, severe patients were also observed to have raised SMN-CE and lower FPN-CE integration additionally. To the best of our knowledge, this is the first study applying a multilayer network model and evaluating multiple dynamic measures to explore the dynamic reconfiguration of the functional brain network following a stroke. We believe these findings could underpin post-stroke functional plasticity and reorganization and may enable new insight into rehabilitation strategies to promote recovery of function.

### *A. Whole Brain Static Modularity Across Stroke Patients with Different Levels of Severity*

In post-stroke patients, the value of static modularity is lower than in healthy controls. This result was consistent with previous studies providing evidence that modularity in resting-state post-stroke patients is reduced [11], [31]. There was no significant group effect detected in stroke patients regarding static modularity, but a much higher value can be observed in severe patients. Despite there being no direct evidence proving that the relationship between modularity and post-stroke severity fits a U-shape of the curve (modularity vs. severity), such a plausible relationship has been depicted in previous dynamic functional connectivity analyses for acute stroke patients. For example, mild patients prefer to stay in a densely connected brain state characterized by a lower level of modularity than severe patients [14]. However, studies on post-stroke recovery also present a linear relationship between modularity and behaviors: modularity continually increases as the severity of clinical symptoms alleviates until it reaches a normal level. Duncan et al. [9] reported that aphasia patients with improved narrative production following therapy had increased modularity. A recent study of large-scale stroke patients by Siegel et al. [31] demonstrated that two weeks after stroke, patients' functional deficits had been alleviated, and in parallel with this function recovery, the modular structure reemerged and was enriched. These two distinctly different trends in modularity can be explained by differences between the between-person and the within-person effects. Within-person effects emphasize the trend over a certain period for a specific group, while between-person effects fuse multiple

This work is licensed under a Creative Commons Attribution-NonCommercial-NoDerivatives 4.0 License. For more information, see https://creativecommons.org/licenses/by-nc-nd/4.0/

This article has been accepted for publication in IEEE Journal of Biomedical and Health Informatics. This is the author's version which has not been fully edited and content may change prior to final publication. Citation information: DOI 10.1109/JBHI.2024.3371097



differences that the groups exhibit [39].

### *B. Functional Segregation and Integration in dynamic reconfiguration of brain function network*

The human brain can be parcelled into various functional domains. Functional segregation refers to the independent processing ability of the locally isolated domain to define specific brain functions (when it comes to cooperation between the distributed domains, it refers to functional integration). The modular brain organization is not static but instead fluctuates constantly in response to brain functional demands, even in a resting state. Hence, it is more reasonable to conclude post-stroke functional segregation and integration trends from the dynamic measures than from the static modularity.

First, there was reduced recruitment within functional networks in both mild and severe patients suggesting that VIS and LN in mild patients, SMN, SAN, and LN in severe patients tend to process information in an isolated state. Given the bodily functional deficits related to these functional domains, this isolation might correlate with the specific severity of clinical symptoms. Particularly, severe patients were found to have significantly lower recruitment in SAN than mild patients, suggesting that patients with higher clinical symptoms have much lower SAN segregation. Next, results show that the pairwise integration between functional domains has been significantly altered. Regardless of patient groups, increased integration between VIS and LN and between DAN and CE, and decreased integration between DMN and CE can be observed. The post-stroke integration changes suggest that the stroke lesions alter the information transfer between domains instead of within the domain. Besides, it is worth noting that severe patients show more integration alteration than mild patients. This alteration presents a link between the interaction-between-domain and the level of post-stroke clinical symptoms, suggesting that between-domain interaction could potentially be a new biomarker for stroke severity. Interestingly, results also show that the between-network interaction alteration follows a specific balancing mechanism: some pairwise integrations increase while others decrease.

Collectively, stroke groups with different severity levels express distinct dynamic patterns, however, for either the mild or severe patients, the recruitment and integration trend suggests a trade-off between network segregation and integration: segregation increases between some systems, and integration increases or decreases between others.

### *C. The Association between Network Flexibility and Stroke Impairment*

As a measure developed on the time-varying network, the flexibility in this study emphasizes the temporal variations in the network configuration. The higher the flexibility, the more frequently the network engages in between network interactions. The lower flexibility found in mild patients indicates that the role of two networks in brain communication is decreasing, which explains the post-stroke cognitive deficit [40]. As there are no networks with significantly different flexibility in severe patients, we can make no conclusions regarding the flexibility level being dependent on the severity level. Nevertheless, network flexibility has been found to be associated with verbal creativity [41], attention [42], fatigue [43], depression [25], and high-order cognitive functions [44]. These studies confirm the neurobiological basis of network flexibility during adaptive brain processes. Hence, it is natural to speculate that flexibility is positively correlated with stroke severity. This alleged relationship supports a post-stroke neuron bypass theory [45], i.e., through network reorganization, the neurons bypass the brain regions with deficits and attempt to form new connectivity. These newly forming pathways drive the switching rate to fluctuate wildly to an optimal connectivity pattern. However, if the flexibility could foresee the exacerbation or improvement of brain function after a stroke still needs to be verified. [46]. In the future, it is worth trying to acquire long-term post-stroke behavioral markers to investigate the link between flexibility and brain function.

### *D. Limitations*

The current research still has some limitations for further consideration. First, the sample size of our study was relatively small; hence, independent studies with large cohorts of patients will be crucial for the validation of our conclusions. Second, we optimized the multilayer modularity with the grid-search method across a range of $\gamma \in [0.9, 1.0, 1.1]$ and $\omega \in [0.5, 0.75, 1.0]$. Such a method has a risk of falling the trap of local optimal. Besides, recent studies suggest that the $\gamma = 1.0$ and $\omega = 2.5$ can achieve the highest test-retest reliability of modularity. The value of $\gamma$ is already in our candidate range and hence a broader range of $\omega$ and more flexible combinations might be worthwhile for future studies. Third, in this study, the brain parcellation of 32 ROIs was only considered, which covers fewer hubs in subcortical regions. Whether subcortical regions have network reconfiguration is still poorly known. In the future, fine-grained brain parcellation such as 264 ROIs provided by Power et al. [47] and 300-ROI parcellation provided by Schaefer et al. [48] can be explored further to enhance the understanding of the readjustment both in the cortical and subcortical networks.

## CONCLUSION

In this study, a multi-layer network analysis-based method was utilized to study the dynamic changes in the brains of stroke patients with different severity levels. The indistinguishable network reconstruction pattern with severity dependencies demonstrates the potential of this dynamic method in capturing essential features of clinical symptoms of a stroke. Patients with severe deficiencies tend to reduce recruitment and increase integration between networks. However, patients with mild defects have lower network flexibility. These observations provide clear evidence for brain network reconstruction after stroke, whereas the static method cannot do. Therefore, this study expands the resting state fMRI-based functional connectivity analysis methods for post-stroke patients. Notably, the degree of functional impairment after stroke seems related to differences in dynamic network reorganization patterns among stroke patients. In clinical practice, these findings could help

This work is licensed under a Creative Commons Attribution-NonCommercial-NoDerivatives 4.0 License. For more information, see https://creativecommons.org/licenses/by-nc-nd/4.0/

This article has been accepted for publication in IEEE Journal of Biomedical and Health Informatics. This is the author's version which has not been fully edited and content may change prior to final publication. Citation information: DOI 10.1109/JBHI.2024.3371097



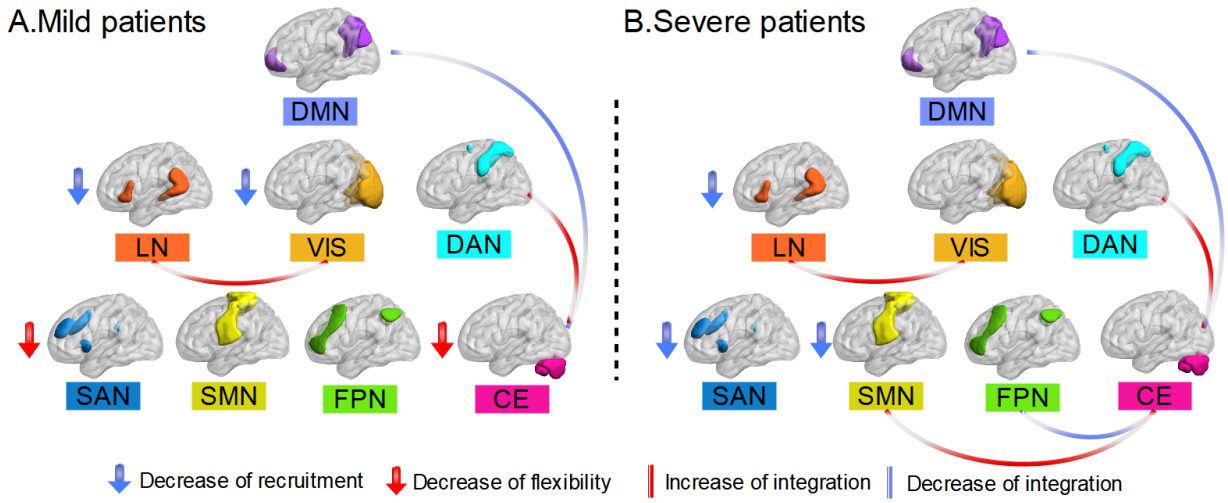


Fig. 7. Summary of the reconfiguration patterns of stroke patients with different degrees of symptoms. **(A)** Mild: a reduction in recruitment in VIS and LN, decreased DMN-CE and increased VIS-LN and DAN-CE integration, and declined SAN and CE flexibility. **(B)** Severe: reduced SMN, SAN, and LN recruitment. In addition to the same integration trend as in mild patients, severe patients were also observed to have raised SMN-CE and lower FPN-CE integration. The legend of corresponding symbols is presented in the figure. DMN: Default mode network. SMN: sensorimotor network. VIS: Visual network. SAN: salience network. DAN: dorsal attention network. FPN: frontoparietal network. LN: language network, CE: cerebellar network.

observe the transition from a severe to a mild state during stroke patients' rehabilitation process. Moreover, the proposed dynamic method could assist clinicians in performing accurate prognosis assessments or be used as a brain status monitoring method while conducting the therapeutic intervention.

## ACKNOWLEDGMENT

The work presented in this paper has been aided by many clinicians and radiologists over the past year. Most notably, The dean of the Department of Radiology, Affiliated Cancer Hospital of Shantou University Medical College, Dr. Aiqun Cai provides a lot of help in the acquisition of MRI scans; the radiologists, Dr. Yao Xie and Dr. Yin Xiao from the Affiliated Cancer Hospital of Shantou University Medical College helped identify the stroke lesion. In addition, Dr. Xiaopu Chen (physician), from the First Affiliated Hospital of Shantou University Medical College has helped in the multiple stages of patient recruitment, fMRI acquisition, and clinical function assessment.

## REFERENCES

[1] M. H. Adhikari et al., "Decreased integration and information capacity in stroke measured by whole brain models of resting state activity," Brain, vol. 140, no. 4, pp. 1068–1085, 2017.

[2] E. Carrera and G. Tononi, "Diaschisis: Past, present, future," Brain, vol. 137, no. 9, pp. 2408–2422, 2014.

[3] O. Sporns and R. F. Betzel, "Modular brain networks," Annual Review of Psychology, vol. 67, p. 613, 2016.

[4] Z. Yang, Q. K. Telesford, A. R. Franco, R. Lim, S. Gu, T. Xu, L. Ai, F. X. Castellanos, C.-G. Yan, and S. Colcombe, "Measurement reliability for individual differences in multilayer network dynamics: Cautions and considerations," NeuroImage, vol. 225, p. 117489, 2021.

[5] O. Sporns, "Network attributes for segregation and integration in the human brain," Current Opinion in Neurobiology, vol. 23, no. 2, pp. 162–171, 2013.

[6] M. Shi, S. Liu, H. Chen, W. Geng, X. Yin, Y.-C. Chen, and L. Wang, "Disrupted brain functional network topology in unilateral acute brainstem ischemic stroke," Brain Imaging and Behavior, vol. 15, no. 1, pp. 444–452, 2021.

[7] L. Wang, C. Yu, H. Chen, W. Qin, Y. He, F. Fan, Y. Zhang, M. Wang, K. Li, and Y. Zang, "Dynamic functional reorganization of the motor execution network after stroke," Brain, vol. 133, no. 4, pp. 1224–1238, 2010.

[8] N. S. Ward, "Restoring brain function after stroke — bridging the gap between animals and humans," Nature Reviews Neurology, vol. 13, no. 4, pp. 244–255, 2017.

[9] E. S. Duncan and S. L. Small, "Increased modularity of resting state networks supports improved narrative production in aphasia recovery," Brain Connectivity, vol. 6, no. 7, pp. 524–529, 2016.

[10] C. Gratton, E. M. Nomura, F. Pérez, and M. D'Esposito, "Focal brain lesions to critical locations cause widespread disruption of the modular organization of the brain," Journal of Cognitive Neuroscience, vol. 24, no. 6, pp. 1275–1285, 2012.

[11] J. S. Siegel, L. E. Ramsey, A. Z. Snyder, N. V. Metcalf, R. V. Chacko, K. Weinberger, A. Baldassarre, C. D. Hacker, G. L. Shulman, and M. Corbetta, "Disruptions of network connectivity predict impairment in multiple behavioral domains after stroke," Proceedings of the National Academy of Sciences, vol. 113, no. 30, pp. E4367–E4376, 2016.

[12] K. Wu, Q. Fang, K. Neville, and B. Jelfs, "Evaluation of module dynamics in functional brain networks after stroke," in 2023 45th Annual International Conference of the IEEE Engineering in Medicine & Biology Society (EMBC). IEEE, 2023, pp. 1–4.

[13] M. E. Newman, "Fast algorithm for detecting community structure in networks," Physical Review E, vol. 69, no. 6, p. 066133, 2004.

[14] A. K. Bonkhoff, F. A. Espinoza, H. Gazula, V. M. Vergara, L. Hensel, J. Michely, T. Paul, A. K. Rehme, L. J. Volz, and G. R. Fink, "Acute ischaemic stroke alters the brain's preference for distinct dynamic connectivity states," Brain, vol. 143, no. 5, pp. 1525–1540, 2020.

[15] M. G. Mattar, M. W. Cole, S. L. Thompson-Schill, and D. S. Bassett, "A functional cartography of cognitive systems," PLoS Computational Biology, vol. 11, no. 12, p. e1004533, 2015.

[16] E. A. Allen, E. Damaraju, S. M. Plis, E. B. Erhardt, T. Eichele, and V. D. Calhoun, "Tracking whole-brain connectivity dynamics in the resting state," Cerebral Cortex, vol. 24, no. 3, pp. 663–676, 2014.

[17] D. J. Lurie, D. Kessler, D. S. Bassett, R. F. Betzel, M. Breakspear, S. Kheilholz, A. Kucyi, R. Liégeois, M. A. Lindquist, and A. R. McIntosh, "Questions and controversies in the study of time-varying functional connectivity in resting fMRI," Network Neuroscience, vol. 4, no. 1, pp. 30–69, 2020.

[18] M. G. Preti, T. A. Bolton, and D. Van De Ville, "The dynamic functional

This work is licensed under a Creative Commons Attribution-NonCommercial-NoDerivatives 4.0 License. For more information, see https://creativecommons.org/licenses/by-nc-nd/4.0/

This article has been accepted for publication in IEEE Journal of Biomedical and Health Informatics. This is the author's version which has not been fully edited and content may change prior to final publication. Citation information: DOI 10.1109/JBHI.2024.3371097



connectome: State-of-the-art and perspectives," NeuroImage, vol. 160, pp. 41–54, 2017.
[19] K. Wu, B. Jelfs, K. Neville, and J. Q. Fang, "fmri-based static and dynamic functional connectivity analysis for post-stroke motor dysfunction patient: A review," arXiv preprint arXiv:2301.07171, 2022.
[20] K. Finc, K. Bonna, X. He, D. M. Lydon-Staley, S. Kühn, W. Duch, and D. S. Bassett, "Dynamic reconfiguration of functional brain networks during working memory training," Nature Communications, vol. 11, no. 1, pp. 1–15, 2020.
[21] S. Tian, Y. Sun, J. Shao, S. Zhang, Z. Mo, X. Liu, Q. Wang, L. Wang, P. Zhao, and M. R. Chattun, "Predicting escitalopram monotherapy response in depression: the role of anterior cingulate cortex," Human Brain Mapping, vol. 41, no. 5, pp. 1249–1260, 2020.
[22] G. Michelini, L. J. Norman, P. Shaw, and S. K. Loo, "Treatment biomarkers for ADHD: Taking stock and moving forward," Translational Psychiatry, vol. 12, no. 1, pp. 1–30, 2022.
[23] G. Gifford, N. Crossley, M. J. Kempton, S. Morgan, P. Dazzan, J. Young, and P. McGuire, "Resting state fMRI based multilayer network configuration in patients with schizophrenia," NeuroImage: Clinical, vol. 25, p. 102169, 2020.
[24] X. He, D. S. Bassett, G. Chaitanya, M. R. Sperling, L. Kozlowski, and J. I. Tracy, "Disrupted dynamic network reconfiguration of the language system in temporal lobe epilepsy," Brain, vol. 141, no. 5, pp. 1375–1389, 2018.
[25] S. Han, Q. Cui, X. Wang, L. Li, D. Li, Z. He, X. Guo, Y. Fan, J. Guo, and W. Sheng, "Resting state functional network switching rate is differently altered in bipolar disorder and major depressive disorder," Human Brain Mapping, vol. 41, no. 12, pp. 3295–3304, 2020.
[26] A. K. Bonkhoff, M. Schirmer, M. Bretzner, M. Etherton, and N. S. Rost, "Abnormal dynamic functional connectivity is linked to recovery after acute ischemic stroke," Human Brain Mapping, no. 3, 2021.
[27] K. Wu, B. Jelfs, S. S. Mahmoud, K. Neville, and J. Q. Fang, "Tracking functional network connectivity dynamics in the elderly," Frontiers in Neuroscience, vol. 17, 2023.
[28] S. Whitfield-Gabrieli and A. Nieto-Castanon, "CONN: A functional connectivity toolbox for correlated and anticorrelated brain networks," Brain Connectivity, vol. 2, no. 3, pp. 125–141, 2012.
[29] W. D. Penny, K. J. Friston, J. T. Ashburner, S. J. Kiebel, and T. E. Nichols, Statistical parametric mapping: the analysis of functional brain images. Elsevier, 2011.
[30] J. S. Siegel, A. Z. Snyder, L. Ramsey, G. L. Shulman, and M. Corbetta, "The effects of hemodynamic lag on functional connectivity and behavior after stroke," Journal of Cerebral Blood Flow & Metabolism, vol. 36, no. 12, pp. 2162–2176, 2016.
[31] J. S. Siegel, B. A. Seitzman, L. E. Ramsey, M. Ortega, E. M. Gordon, N. U. Dosenbach, S. E. Petersen, G. L. Shulman, and M. Corbetta, "Re-emergence of modular brain networks in stroke recovery," Cortex, vol. 101, pp. 44–59, 2018.
[32] M. Rubinov and O. Sporns, "Complex network measures of brain connectivity: Uses and interpretations," NeuroImage, vol. 52, no. 3, pp. 1059–1069, 2010.
[33] C. Favaretto, M. Allegra, G. Deco, N. V. Metcalf, J. C. Griffis, G. L. Shulman, A. Brovelli, and M. Corbetta, "Subcortical-cortical dynamical states of the human brain and their breakdown in stroke," Nature Communications, vol. 13, no. 1, pp. 1–17, 2022.
[34] H. Liu, K. Hu, Y. Peng, X. Tian, M. Wang, B. Ma, Y. Wu, W. Sun, B. Liu, A. Li et al., "Dynamic reconfiguration of human brain networks across altered states of consciousness," Behavioural Brain Research, vol. 419, p. 113685, 2022.
[35] D. S. Bassett, M. A. Porter, N. F. Wymbs, S. T. Grafton, J. M. Carlson, and P. J. Mucha, "Robust detection of dynamic community structure in networks," Chaos: An Interdisciplinary Journal of Nonlinear Science, vol. 23, no. 1, p. 013142, 2013.
[36] P. J. Mucha et al., "Community structure in time-dependent, multiscale, and multiplex networks," Science, vol. 328, no. 5980, pp. 876–878, 2010.
[37] D. S. Bassett, M. Yang, N. F. Wymbs, and S. T. Grafton, "Learning-induced autonomy of sensorimotor systems," Nature Neuroscience, vol. 18, no. 5, pp. 744–751, 2015.
[38] S. Maslov and K. Sneppen, "Specificity and stability in topology of protein networks," Science, vol. 296, no. 5569, pp. 910–913, 2002.
[39] P. J. Curran and D. J. Bauer, "The disaggregation of within-person and between-person effects in longitudinal models of change," Annual Review of Psychology, vol. 62, p. 583, 2011.
[40] B. Rao, S. Wang, M. Yu, L. Chen, G. Miao, X. Zhou, H. Zhou, W. Liao, and H. Xu, "Suboptimal states and frontoparietal network-centered incomplete compensation revealed by dynamic functional network connectivity in patients with post-stroke cognitive impairment," Frontiers in Aging Neuroscience, vol. 14, 2022.
[41] Q. Feng, L. He, W. Yang, Y. Zhang, X. Wu, and J. Qiu, "Verbal creativity is correlated with the dynamic reconfiguration of brain networks in the resting state," Frontiers in Psychology, vol. 10, p. 894, 2019.
[42] J. M. Shine, O. Koyejo, and R. A. Poldrack, "Temporal metastates are associated with differential patterns of time-resolved connectivity, network topology, and attention," Proceedings of the National Academy of Sciences, vol. 113, no. 35, pp. 9888–9891, 2016.
[43] R. F. Betzel, T. D. Satterthwaite, J. I. Gold, and D. S. Bassett, "Positive affect, surprise, and fatigue are correlates of network flexibility," Scientific Reports, vol. 7, no. 1, pp. 1–10, 2017.
[44] M. Pedersen, A. Zalesky, A. Omidvarnia, and G. D. Jackson, "Multilayer network switching rate predicts brain performance," Proceedings of the National Academy of Sciences, vol. 115, no. 52, pp. 13 376–13 381, 2018.
[45] A. Crofts, M. E. Kelly, and C. L. Gibson, "Imaging functional recovery following ischemic stroke: Clinical and preclinical fMRI studies," Journal of Neuroimaging, vol. 30, no. 1, pp. 5–14, 2020.
[46] C. L. Gallen and M. D'Esposito, "Brain modularity: A biomarker of intervention-related plasticity," Trends in Cognitive Sciences, vol. 23, no. 4, pp. 293–304, 2019.
[47] J. D. Power, A. L. Cohen, S. M. Nelson, G. S. Wig, K. A. Barnes, J. A. Church, A. C. Vogel, T. O. Laumann, F. M. Miezin, B. L. Schlaggar et al., "Functional network organization of the human brain," Neuron, vol. 72, no. 4, pp. 665–678, 2011.
[48] A. Schaefer, R. Kong, E. M. Gordon, T. O. Laumann, X.-N. Zuo, A. J. Holmes, S. B. Eickhoff, and B. T. Yeo, "Local-global parcellation of the human cerebral cortex from intrinsic functional connectivity mri," Cerebral cortex, vol. 28, no. 9, pp. 3095–3114, 2018.

This work is licensed under a Creative Commons Attribution-NonCommercial-NoDerivatives 4.0 License. For more information, see https://creativecommons.org/licenses/by-nc-nd/4.0/